

Radiographic identification of the primary structures of the ankle syndesmosis

Brady T. Williams¹ · Evan W. James¹ · Kyle A. Jisa¹ · C. Thomas Haytmanek^{1,2} · Robert F. LaPrade^{1,2} · Thomas O. Clanton^{1,2}

Received: 18 March 2015 / Accepted: 28 July 2015 / Published online: 21 August 2015
© European Society of Sports Traumatology, Knee Surgery, Arthroscopy (ESSKA) 2015

Abstract

Purpose The purpose of this study was to quantitatively describe the locations of the syndesmotic ligaments and the tibiofibular articulating cartilage surfaces on standard radiographic views using reproducible radiographic landmarks and reference axes.

Methods Twelve non-paired ankles were dissected to identify the anterior–inferior tibiofibular ligament (AITFL), posterior–inferior tibiofibular ligament (PITFL), interosseous tibiofibular ligament (ITFL), and the cartilage surfaces of the syndesmosis. Structures were marked with 2-mm radiopaque spheres prior to obtaining lateral and mortise radiographs. Measurements were performed by two independent raters to assess intra- and interobserver reliability via intraclass correlation coefficients (ICCs).

Results Measurements demonstrated excellent agreement between observers and across trials (all ICCs ≥ 0.960). On the lateral view, the AITFL tibial origin was 9.6 ± 1.5 mm superior and posterior to the anterior tibial plafond. Its fibular insertion was 4.4 ± 1.7 mm superior and posterior to the anterior fibular tubercle. The centre of the tibial cartilage facet of the tibiofibular contact zone was 8.4 ± 2.1 mm posterior and superior to the anterior plafond. The proximal and distal aspects of the ITFL tibial attachment were 45.9 ± 7.9 and 12.4 ± 3.4 mm proximal to the central plafond, respectively. The superficial and deep PITFL coursed anterior and distally from the posterior tibia to fibula. On the mortise view, the AITFL tibial attachment centre was 5.6 ± 2.4 mm lateral and superior to the lateral extent of

the plafond (4.3 mm lateral, 3.3 mm superior), and its fibular insertion was 21.2 ± 2.1 mm superior and medial to the inferior tip of the lateral malleolus.

Conclusions Quantitative radiographic guidelines describing the locations of the primary syndesmotic structures demonstrated excellent reliability and reproducibility. Defined guidelines provide additional clinically relevant information regarding the radiographic anatomy of the syndesmosis and may assist with preoperative planning, augment intraoperative navigation, and provide additional means for objective postoperative assessment.

Keywords Ankle · High ankle sprains · Anterior–inferior tibiofibular ligament · Posterior–inferior tibiofibular ligament · Interosseous tibiofibular ligament

Introduction

The ankle syndesmosis is a fibrous articulation joining the distal tibia and fibula that is stabilized by three ligaments including the anterior–inferior tibiofibular ligament (AITFL), posterior–inferior tibiofibular ligament (PITFL), and interosseous tibiofibular ligament (ITFL) [1, 10, 44]. The space between the tibia and fibula form the synovial recess which contains the direct articulating cartilage surfaces of the tibia and fibula, described previously as the tibiofibular contact zone [1, 10, 44]. Together, these elements comprise the primary structures of the ankle syndesmosis.

Sprains of the ankle syndesmosis, commonly called high ankle sprains, account for as much as 25 % of all ankle sprains in athletic patient populations [19]. Most isolated sprains of the syndesmosis may be treated non-operatively; however, syndesmosis injuries can often result in prolonged periods of pain and functional limitations [7, 13, 17, 39].

✉ Thomas O. Clanton
tclanton@thesteadmanclinic.com

¹ Department of BioMedical Engineering, Steadman Philippon Research Institute, Vail, CO, USA

² The Steadman Clinic, Vail, CO, USA

Furthermore, patients with tibial or fibular fractures and concomitant syndesmotic sprains, or patients with grade III acute or chronic syndesmotic instability often require surgical treatment ranging from proximally placed indirect fixation (screws or suture-button constructs) to allograft reconstruction. Previous clinical outcome studies have correlated anatomic reduction of the syndesmosis with improved clinical outcomes following surgery [30, 37]. Despite this caveat, malreduction is common and current methods to confirm an anatomic reduction are not always accurate whether that be through routine radiographs, fluoroscopy, or stress radiographs [5, 6, 8, 11, 12, 18, 23, 31].

Anatomic reduction is predicated on accurate identification of native syndesmosis anatomy. Recent cadaveric studies have outlined qualitative and quantitative descriptions of syndesmosis anatomy for use during anatomic-based surgical repair and reconstruction procedures [1, 10, 44]. However, radiographic guidelines detailing the anatomic attachments of the syndesmotic ligaments and location of the syndesmotic articular cartilage surfaces are currently lacking. Radiographic guidelines would augment current diagnostic approaches, improve preoperative planning, assist with intraoperative identification of native anatomy, and facilitate objective postoperative assessment of anatomic-based reduction, repair, and reconstruction techniques. Radiographic data describing the anatomic locations of the structures of the syndesmosis may be particularly useful in revision cases or those with concomitant injury where other anatomic landmarks and navigation techniques may be more difficult to interpret.

Therefore, the purpose of this study was to establish qualitative and quantitative radiographic guidelines for identifying the tibial and fibular attachments of the three syndesmotic ligaments and the articulating surfaces of the syndesmosis using standard ankle radiographic views. It was hypothesized that these sites could be reproducibly defined in relation to osseous landmarks and superimposed radiographic axes.

Materials and methods

Twelve non-paired, fresh-frozen cadaveric specimens (mean age 56, range 38–82 years; 4 females and 8 males; 8 left and 4 right) with no history of ankle injury, surgery, osteoarthritis, or significant anatomic abnormalities were used in this study. This sample size was based on similar previously published research [16]. De-identified cadaveric specimens are exempt from Institutional Review Board (IRB) review at our institution; therefore, IRB approval was not required for this study. The relative anatomic positions of the tibia and fibula were preserved using rigid screw fixation placed 10 and 15 cm proximal to the tibiotalar joint

line. Soft tissue dissections were subsequently performed to identify the origin and insertion sites of the AITFL, PITFL, and ITFL in accordance with previous anatomic literature [1, 10, 44]. The three syndesmotic ligaments were sequentially transected at their midsubstance. Tibial and fibular ligamentous remnants were then used to identify the tibial and fibular attachment sites or footprints. The centres of the AITFL and PITFL footprints were identified and marked by shallowly embedding a 2-mm stainless steel sphere (diameter: 2.0 ± 0.0025 mm, sphericity: 0.0006 mm, Small Parts, Inc., Logansport, IN) similar to a previously described technique [16]. Due to the multifascicular nature and/or broad sites of attachment of the AITFL and PITFL, additional 2-mm stainless steel spheres were placed at the superior and inferior bands/margins of each origin and insertion. For the AITFL, this included 2-mm spheres placed in the proximal and distal accessory band(s) (Bassett's Ligament) [2, 44]. For the PITFL, this included the proximal and distal borders of the superficial PITFL in addition to tibial and fibular footprint centres of the deep PITFL fibres (inferior transverse tibiofibular ligament). For the ITFL, the proximal and distal extents of the tibial and fibular fibre attachments were marked using the same technique. Stainless steel spheres were also embedded in the centre of the tibial and fibular cartilage-covered articulating facets, described previously as the tibiofibular contact zone [1, 10, 44]. To ensure that individual spheres could be distinguished in the event of overlap on mortise and lateral radiographs, spheres were placed sequentially from anterior to posterior in each ligament/structure with sequential radiographs obtained at these intervals. Sequential mortise and lateral radiographs were superimposed and compared to accurately identify the individual metallic spheres representing each respective component (AITFL, ITFL, PITFL, Tibiofibular contact zone) of the ankle syndesmosis.

Data collection

Standard lateral and mortise radiographs of each specimen were obtained using a fluoroscopic mini-C-arm (Hologic, Inc., Bedford, MA). Images were obtained under live fluoroscopy to obtain true lateral and mortise views [27]. Lateral view radiographs were defined by an X-ray beam coincident with the intermalleolar axis and superimposition of the medial and lateral profiles of the talar dome. Mortise view radiographs were defined by an X-ray beam perpendicular to the intermalleolar axis and clear visualization of the talofibular joint space. A 25.4-mm-diameter radiopaque stainless steel sphere (diameter: 25.4 ± 0.00254 mm, sphericity: 0.00061 mm, Small Parts, Inc., Logansport, IN) placed at the level of the ankle joint was utilized in all radiographs for measurement calibration and to adjust for any

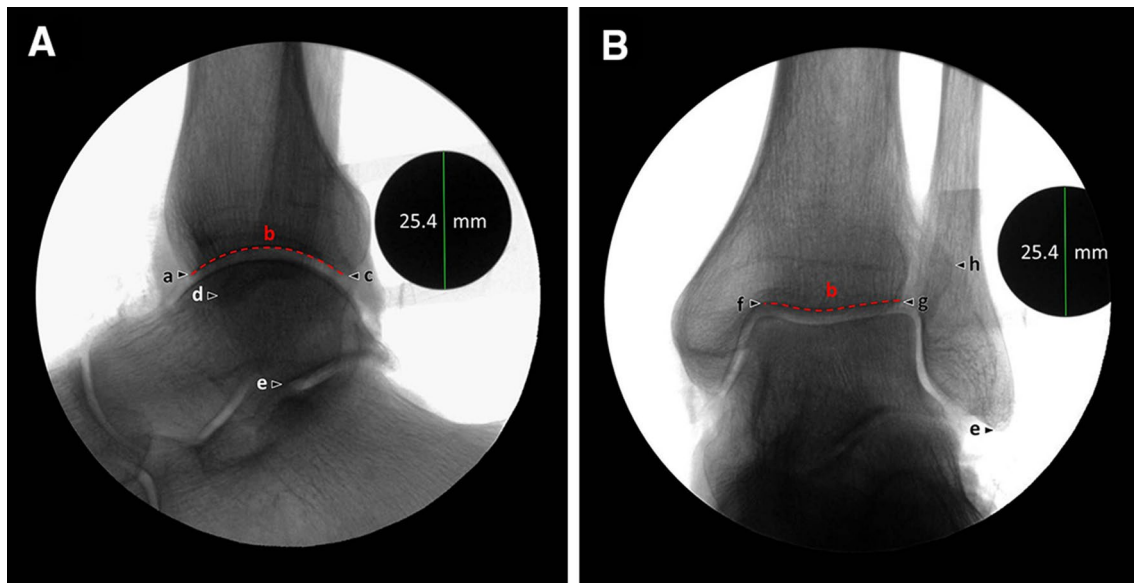


Fig. 1 Representative **A** lateral and **B** mortise radiographic views with labelled reference landmarks used to quantitatively characterize the locations of individual syndesmotic structures. *a* Anterior tibial plafond; *b* tibial plafond; *c* posterior tibial plafond; *d* anterior fibu-

lar tubercle; *e* inferior tip of the lateral malleolus; *f* medial corner of the tibial plafond; *g* lateral corner of the tibial plafond; *h* most lateral tibial point

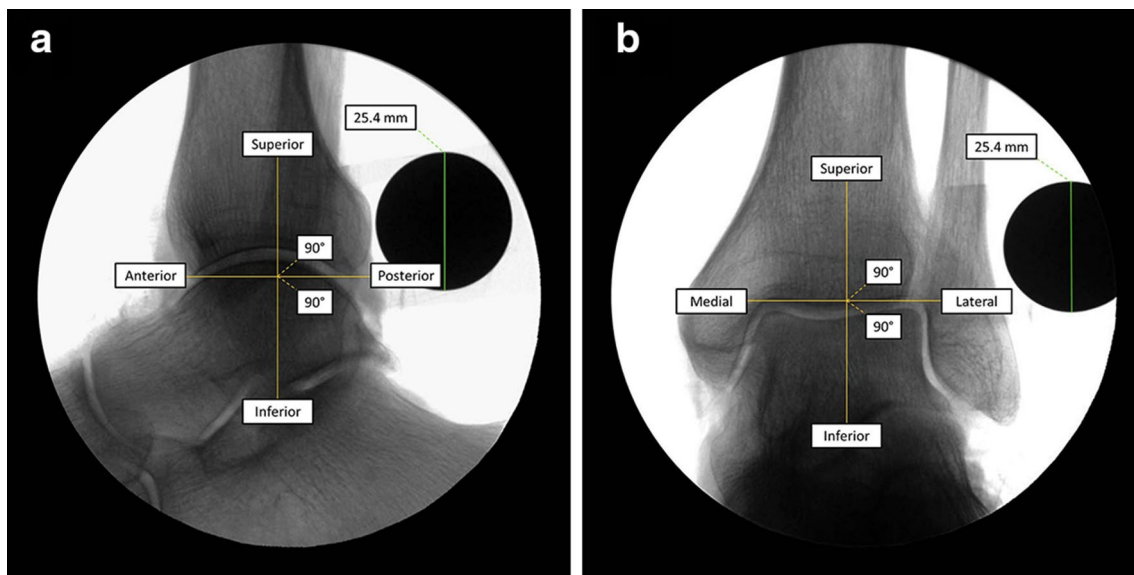


Fig. 2 Representative **a** lateral and **b** mortise radiographic views demonstrating the axes used for radiographic measurements

differences in magnification caused by variation in specimen distance from the X-ray source [16].

Radiographic images were then imported into a picture archiving and communication system (PACS) for measurements (eFilm Workstation® 3.4, Merge Healthcare Inc., Chicago, IL). Radiographic landmarks were selected, and measurements were taken under the direction of a foot and ankle fellowship trained orthopaedic surgeon and the senior

author (TOC). These radiographic landmarks are depicted in Fig. 1. The medial–lateral axis for mortise views and anterior–posterior axis for lateral views were defined by a superimposed reference line parallel to and at the level of the tibial plafond (Fig. 2). The superior–inferior axis was defined by a superimposed reference line perpendicular to the tibial plafond reference line and coincident with the long axis of the tibia [16].

Table 1 Radiographic measurements of the anterior–inferior tibiofibular ligament, lateral view

	Absolute distance (mm)	Directionality (mm) ^a	
	Mean ± SD	Anterior(+)/posterior(–) Mean	Superior(+)/inferior(–) Mean
Distance between attachments (tibia → fibula)			
Proximal accessory band(s)	3.8 ± 0.8	–3.0	–1.0
Primary band(s)	6.5 ± 1.7	–2.8	–5.7
Distal accessory (Bassett's) band	11.3 ± 3.1	–6.3	–8.9
Width of ligament attachment (proximal → distal)			
Tibial attachment	14.7 ± 1.6	6.9	–12.7
Fibular attachment	21.0 ± 3.8	3.9	–20.4
Tibial attachment to anterior tibial plafond			
Proximal accessory band(s)	17.7 ± 2.2	6.4	–16.1
Primary band(s)	9.6 ± 1.5	2.8	–8.8
Distal accessory (Bassett's) band	4.0 ± 1.9	–0.5	–3.5
Fibular attachment to anterior fibular tubercle			
Proximal accessory band(s)	16.7 ± 3.3	6.1	–15.2
Primary band(s)	4.4 ± 1.7	2.2	–3.5
Distal accessory (Bassett's) band	5.9 ± 2.6	2.6	5.0
Fibular attachment to inferior tip of the lateral malleolus			
Proximal accessory band(s)	32.4 ± 4.1	–6.1	–31.4
Primary band(s)	22.5 ± 3.0	–10.0	–19.8
Distal accessory (Bassett's) band	15.0 ± 4.0	–9.7	–11.1

^a Directionality components were averaged and reported for each measurement starting from each respective attachment to the landmark of interest

Statistical analyses

Measurements were taken by two independent observers with varying levels of medical training to calculate interobserver reliability (BTW, KAJ). Measurements included the mean absolute distance in addition to the mean superior–inferior component, and the mean anterior–posterior (lateral view) or medial–lateral (mortise view) component of each distance. Agreement between reviewers and across trials was assessed via 2-way mixed, random measure intraclass correlation coefficients (ICCs) for each ligament/structure and radiographic view [38]. Statistical analyses were performed using SPSS Statistics, version 20 (SPSS Inc, an IBM Company). For calculation of the intraobserver ICCs, the primary reviewer (BTW) performed measurements twice separated by a minimum interval of 2 weeks to reduce the potential for recall bias.

Results

Lateral radiographic view

Select distances from each syndesmotic structure to individual radiographic landmarks on the lateral view

are reported in Tables 1, 2 and 3 as means and standard deviations and visually represented in Figs. 1A, 3a, 4a and 5a. Both interobserver and intraobserver ICCs demonstrated excellent agreement between raters and reproducibility across trials for all structures of the syndesmosis on lateral radiographic views (Tables 4, 5).

On the lateral view (Fig. 3a), the AITFL tibial attachment was superior and slightly posterior to the anterior corner of the tibial plafond, while the AITFL fibular footprint centre was superior and posterior to the anterior-most point of the anterior fibular tubercle. The superficial PITFL (Fig. 4a) footprint centre was superior to the posterior corner of the tibial plafond, while the deep PITFL attached further distally and anteriorly. The ITFL (Fig. 5a) had a broad tibial attachment, extending from 45.9 ± 7.9 mm proximal to the joint line to 12.4 ± 3.4 mm proximal to the joint line as measured in line with the long axis of the tibia. Distal to the inferior margin of the ITFL, a synovial-lined joint space, which contained areas of tibial and fibular articulating cartilage (Fig. 5a), termed the syndesmotic tibiofibular contact zone, were found in all specimens. The centre of the tibial articulating cartilage was posterior and superior to the anterior corner of the tibial plafond.

Table 2 Radiographic measurements of the posterior–inferior tibiofibular ligament, lateral view

	Absolute distance (mm) Mean \pm SD	Directionality (mm) ^a	
		Anterior(+)/posterior(-) Mean	Superior(+)/inferior(-) Mean
<i>Superficial fibres</i>			
Distance between attachments (tibia \rightarrow fibula)			
Proximal border	4.9 \pm 1.8	2.4	-3.8
Centre	5.4 \pm 2.1	3.3	-3.7
Distal border	7.4 \pm 2.3	3.7	-5.9
Width of ligament attachment (proximal \rightarrow distal)			
Tibial attachment	10.3 \pm 1.8	-2.9	-9.7
Fibular attachment	11.6 \pm 2.4	-1.0	-11.3
Tibial attachment to posterior tibial plafond			
Proximal border	13.6 \pm 2.0	-1.5	-13.1
Centre	7.4 \pm 1.6	0.7	-6.9
Distal border	4.1 \pm 1.4	1.0	-3.4
Fibular attachment to inferior tip of the lateral malleolus			
Proximal border	27.1 \pm 2.7	9.5	-25.0
Centre	22.0 \pm 2.3	10.5	-19.0
Distal border	17.4 \pm 2.0	10.5	-13.4
<i>Deep fibres</i>			
Distance between attachments (tibia \rightarrow fibula)			
Tibial attachment to posterior tibial plafond	8.3 \pm 3.1	6.5	-4.6
Fibular attachment to inferior tip of the lateral malleolus	3.2 \pm 1.5	-0.5	-2.6
Fibular attachment to inferior tip of the lateral malleolus	15.4 \pm 3.4	6.4	-13.5

^a Directionality components were averaged and reported for each measurement starting from each respective attachment to the landmark of interest

Table 3 Radiographic measurements of the interosseous tibiofibular ligament and tibiofibular contact zone, lateral view

	Absolute distance (mm) Mean \pm SD	Directionality (mm) ^a	
		Anterior(+)/posterior(-) Mean	Superior(+)/inferior(-) Mean
<i>Interosseous tibiofibular ligament</i>			
Width of ligament attachment (proximal \rightarrow distal)			
Tibial attachment	33.8 \pm 6.9	-3.9	-33.4
Fibular attachment	31.9 \pm 5.2	-0.8	-31.7
Tibial attachment to tibial plafond (along superior–inferior axis)			
Proximal terminus	45.9 \pm 7.9	0.0	-45.9
Distal terminus	12.4 \pm 3.4	0.0	-12.4
Fibular attachment to inferior tip of the lateral malleolus			
Proximal terminus	58.7 \pm 5.6	-0.5	-58.4
Distal terminus	27.0 \pm 3.2	0.3	-26.6
<i>Tibiofibular contact zone</i>			
Tibial cartilage facet to anterior tibial plafond	8.4 \pm 2.1	5.9	-5.3
Fibular cartilage facet to inferior tip of the lateral malleolus	21.3 \pm 2.5	-8.3	-19.3

^a Directionality components were averaged and reported for each measurement starting from each respective attachment to the landmark of interest

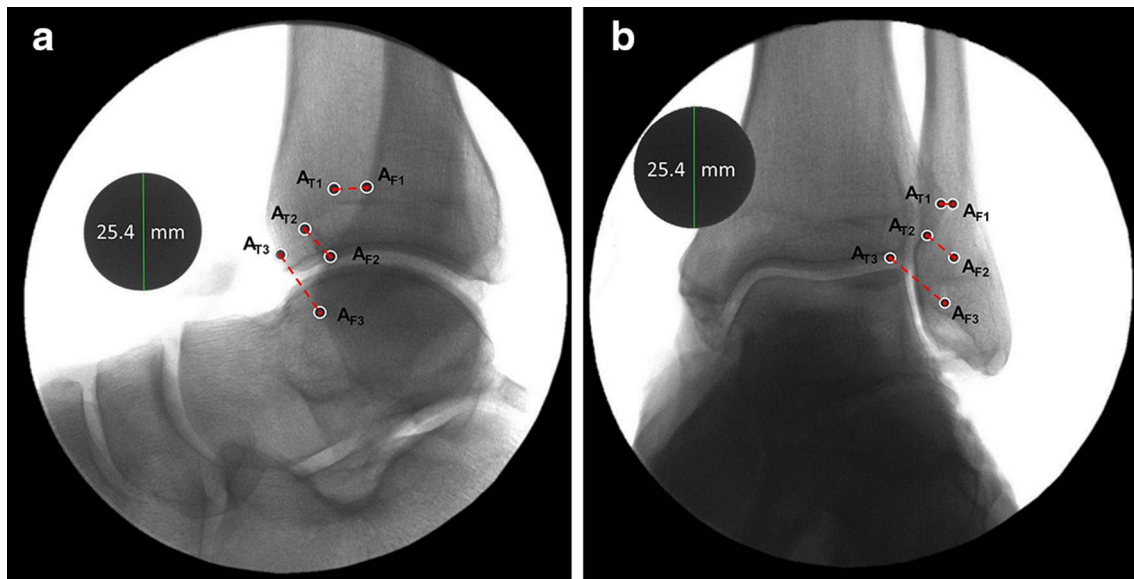


Fig. 3 Representative **a** lateral and **b** mortise radiographic views demonstrating the attachment sites of the anterior–inferior tibiofibular ligament (AITFL), including the tibial and fibular attachment centres

of the proximal accessory bands (A_{T1}/A_{F1}), primary bands (A_{T2}/A_{F2}), and the distal accessory (Basset’s ligament) band (A_{T3}/A_{F3})

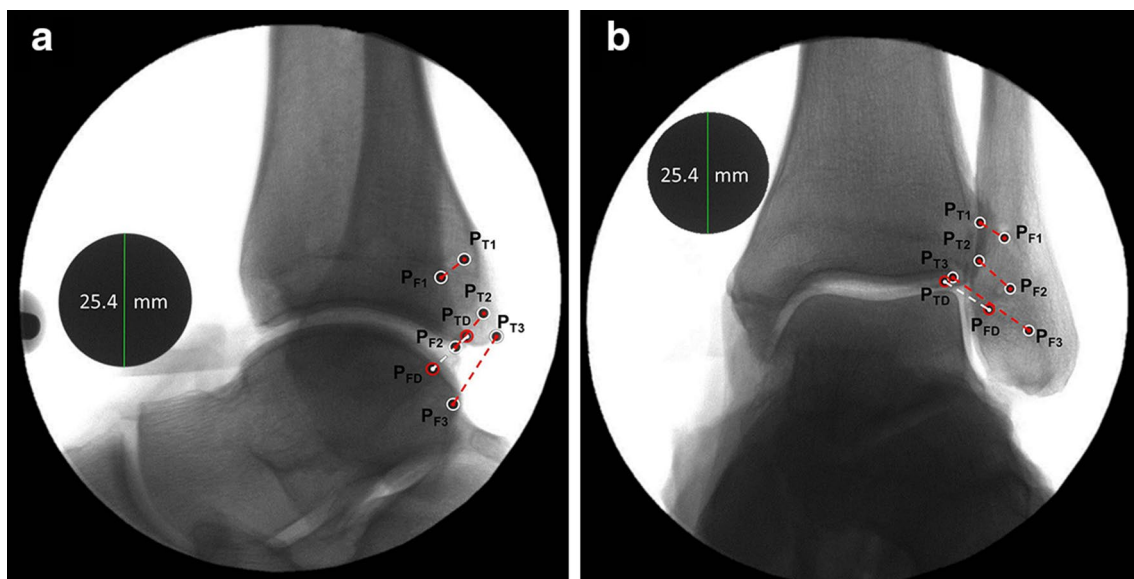


Fig. 4 Representative **a** lateral and **b** mortise radiographic views demonstrating the posterior–inferior tibiofibular ligament (PITFL) attachment sites including the superficial and deep components. The proximal (P_{T1}/P_{F1}) and distal (P_{T3}/P_{F3}) margins of the superficial

PITFL are indicated in addition to its tibial and fibular footprint centres (P_{T2}/P_{F2}). The centres of the tibial and fibular deep attachments are also labelled (P_{TD}/P_{FD})

Mortise radiographic view

Relevant distances from each syndesmotic structure to select radiographic landmarks on the mortise view are listed in Tables 6, 7 and 8 as means and standard deviations and can be visualized in Figs. 1B, 3b, 4b and 5b.

Interobserver and intraobserver ICCs both demonstrated excellent agreement between raters and reproducibility across trials for all structures of the syndesmosis on mortise views (Tables 4, 5).

On the mortise view, the AITFL (Fig. 3b) coursed distally and laterally from its tibial origin, which was lateral

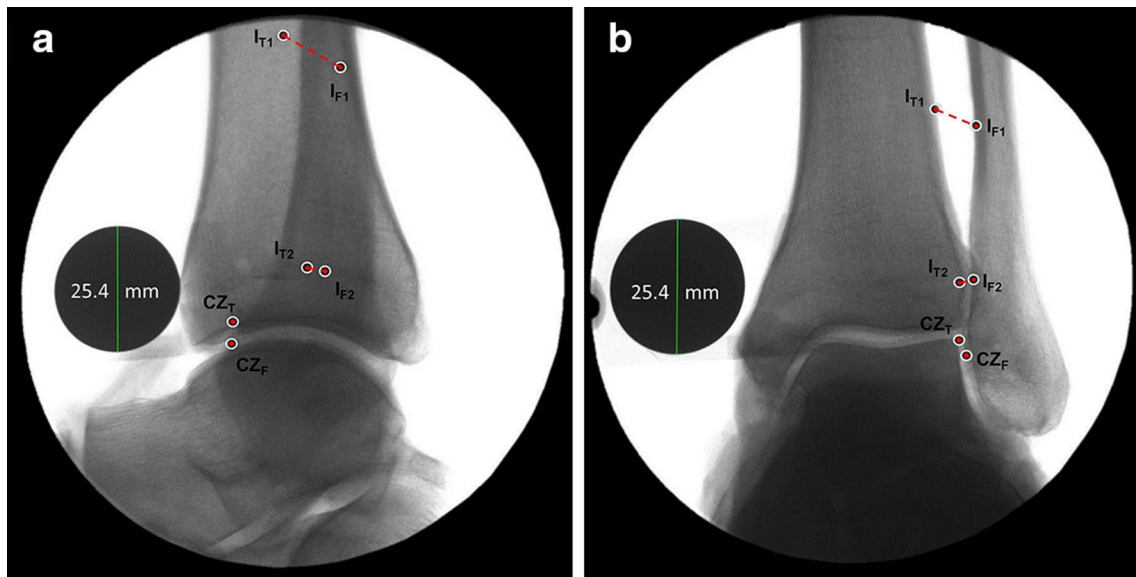


Fig. 5 Representative **a** lateral and **b** mortise radiographic views demonstrating the proximal (I_{T1}/I_{F1}) and distal (I_{T2}/I_{F2}) extents of the tibial and fibular attachments of the interosseous tibiofibular

(ITFL) in addition to the articular cartilage facets (CZ_T/CZ_F) of the tibiofibular contact zone

Table 4 Interobserver reliability

Structure	Lateral view			Mortise view		
	ICC	LB	UB	ICC	LB	UB
AITFL	0.975	0.968	0.981	0.988	0.984	0.991
PITFL	0.984	0.980	0.988	0.989	0.986	0.991
ITFL	0.998	0.996	0.999	0.998	0.995	0.999
CZ	0.977	0.945	0.990	0.983	0.957	0.993

AITFL anterior–inferior tibiofibular ligament, PITFL posterior–inferior tibiofibular ligament, ITFL interosseous tibiofibular ligament, CZ tibiofibular contact zone, ICC intraclass correlation coefficient, LB lower bound, UB upper bound

Table 5 Intraobserver reproducibility

Structure	Lateral view			Mortise view		
	ICC	LB	UB	ICC	LB	UB
AITFL	0.980	0.974	0.984	0.996	0.995	0.997
PITFL	0.983	0.978	0.987	0.996	0.995	0.997
ITFL	0.995	0.992	0.997	0.999	0.999	1.000
CZ	0.960	0.908	0.983	0.998	0.996	0.999

AITFL anterior–inferior tibiofibular ligament, PITFL posterior–inferior tibiofibular ligament, ITFL interosseous tibiofibular ligament, CZ tibiofibular contact zone, ICC intraclass correlation coefficient, LB lower bound, UB upper bound

and superior to the lateral corner of the tibial plafond. The PITFL (Fig. 4b) coursed distally and laterally from its tibial origin to fibular insertion. The centre of the superficial PITFL tibial footprint was medial and superior to the lateral corner of the tibial plafond and attached to the fibula superior and medial to the inferior tip of the lateral

malleolus. The deep fibres originated on the tibia, distal and medial to the centre of the superficial attachment, and inserted distally and medially to the superficial attachment on the fibula. The proximal aspect of the ITFL tibial attachment was located 45.0 ± 9.9 mm proximal to the plafond, while the distal aspect was found 11.1 ± 3.5 mm proximal

Table 6 Radiographic measurements of the anterior–inferior tibiofibular ligament, mortise view

	Absolute distance (mm) Mean \pm SD	Directionality (mm) ^a	
		Lateral(+)/medial(-) Mean	Superior(+)/inferior(-) Mean
Distance between attachments (tibia \rightarrow fibula)			
Proximal accessory band(s)	4.8 \pm 1.2	4.0	-1.9
Primary band(s)	8.4 \pm 1.5	5.5	-5.9
Distal accessory (Bassett's) band	14.1 \pm 2.2	9.9	-9.8
Width of ligament attachment (proximal \rightarrow distal)			
Tibial attachment	14.1 \pm 1.9	-6.7	-11.9
Fibular attachment	20.5 \pm 4.1	-1.1	-20.3
Tibial attachment to lateral corner of the tibial plafond			
Proximal accessory band(s)	12.0 \pm 2.1	-5.9	-10.1
Primary band(s)	5.6 \pm 2.4	-4.3	-3.3
Distal accessory (Bassett's) band	3.1 \pm 1.4	1.5	2.3
Tibial attachment to most lateral tibial point			
Proximal accessory band(s)	3.3 \pm 1.3	2.3	-2.1
Primary band(s)	6.5 \pm 1.8	3.9	4.8
Distal accessory (Bassett's) band	13.6 \pm 1.8	8.9	10.0
Fibular attachment to lateral fibular border (along medial–lateral axis)			
Proximal accessory band(s)	5.8 \pm 1.5	5.8	0.0
Primary band(s)	8.3 \pm 2.2	8.3	0.0
Distal accessory (Bassett's) band	10.9 \pm 2.0	10.9	0.0
Fibular attachment to inferior tip of the lateral malleolus			
Proximal accessory band(s)	32.2 \pm 4.7	4.9	-31.6
Primary band(s)	21.2 \pm 2.1	5.1	-20.3
Distal accessory (Bassett's) band	13.1 \pm 3.1	5.9	-11.4

^a Directionality components were averaged and reported for each measurement starting from each respective attachment to the landmark of interest

to the tibial plafond (Fig. 5b). The cartilage facets of the syndesmotic tibiofibular contact zone were located along the lateral most aspect of the joint line at the intersection of the tibiofibular articulation, just lateral and slightly superior to the superior-lateral corner of the talar dome (Fig. 5b).

Discussion

The most important finding of this study was that the individual ligamentous and articular structures of the ankle syndesmosis were consistently identifiable with respect to anatomically defined and reproducible radiographic landmarks on both standard lateral and mortise radiographic projections. Additionally, measurements demonstrated excellent interobserver and intraobserver agreement for all structures of the syndesmosis on both lateral and mortise radiographic views. Quantitative attachment locations may be particularly useful in guiding surgical fixation in addition to facilitating continued development of anatomically-based surgical repairs and reconstructions.

The radiographic findings presented in this study correlated well with current anatomic descriptions in the literature. Bartonicek [1] reported that the superior extent of the ITFL was located 4–5 cm proximal to the joint line and the distal extent was located at 1–1.5 cm proximal to the tibial plafond. Subsequently, Ebraheim [10] reported corresponding measurements of 32.43 \pm 4.11 and 8.10 \pm 3.35 mm. Most recently, Williams et al. [44] reported the ITFL superior and inferior extents to be 49.4 [95 % confidence interval (CI) 45.4, 53.3] and 9.3 mm (95 % CI 8.3, 10.2) proximal to the central aspect of the tibial plafond. In the present radiographic investigation, the superior extent of the ITFL was located 45.9 \pm 7.9 mm proximal and the distal extent was located at 12.4 \pm 3.4 mm proximal to the tibial plafond on the lateral radiographic view. Similar distances were reported for the mortise view. Radiographic guidelines describing the location of the cartilage facets of the syndesmotic tibiofibular contact zone also correlated with anatomic descriptions. Williams et al. [44] reported the centre of the tibial cartilage facet to be 5.2 mm (95 % CI 4.6, 5.8) posterior to the anterolateral corner of the tibial plafond,

Table 7 Radiographic measurements of the posterior–inferior tibiofibular ligament, mortise view

	Absolute distance (mm) Mean \pm SD	Directionality (mm) ^a	
		Lateral(+)/medial(-) Mean	Superior(+)/inferior(-) Mean
<i>Superficial fibres</i>			
Distance between attachments (tibia \rightarrow fibula)			
Proximal border	8.5 \pm 2.1	6.9	-4.4
Centre	10.4 \pm 1.5	8.1	-4.4
Distal border	17.4 \pm 3.8	16.0	-6.2
Width of ligament attachment (proximal \rightarrow distal)			
Tibial attachment	12.2 \pm 2.3	-7.8	-8.8
Fibular attachment	11.0 \pm 2.2	1.1	-10.5
Tibial attachment to lateral tibial plafond			
Proximal border	7.0 \pm 1.5	-0.1	-6.7
Centre	2.7 \pm 1.7	2.2	-0.9
Distal border	8.4 \pm 1.7	7.9	2.1
Tibial attachment to medial tibial plafond			
Proximal border	27.1 \pm 2.4	-25.9	-6.9
Centre	23.9 \pm 2.4	-23.5	-1.3
Distal border	18.1 \pm 2.4	-17.8	1.9
Tibial attachment to most lateral tibial point			
Proximal border	8.5 \pm 1.2	8.1	1.1
Centre	12.8 \pm 1.8	10.4	6.8
Distal border	19.3 \pm 2.4	16.2	9.9
Fibular attachment to lateral fibular border (along medial–lateral axis)			
Proximal border	10.4 \pm 1.9	10.4	0.0
Centre	11.6 \pm 1.8	11.6	0.0
Distal border	11.2 \pm 3.1	11.2	0.0
Fibular attachment to inferior tip of the lateral malleolus			
Proximal border	27.0 \pm 3.0	7.8	-25.5
Centre	21.5 \pm 3.2	8.0	-19.5
Distal border	16.9 \pm 2.5	7.0	-14.9
<i>Deep fibres</i>			
Distance between attachments (tibia \rightarrow fibula)			
Tibial attachment to lateral tibial plafond	7.3 \pm 2.7	6.2	2.9
Tibial attachment to medial tibial plafond	20.0 \pm 4.2	-19.6	2.8
Tibial attachment to most lateral tibial point	18.5 \pm 2.7	14.4	10.8
Fibular attachment to lateral fibular border (along medial–lateral axis)	15.5 \pm 1.9	15.5	0.0
Fibular attachment to inferior tip of the lateral malleolus	18.9 \pm 3.4	10.9	-15.1

^a Directionality components were averaged and reported for each measurement starting from each respective attachment to the landmark of interest

while the present radiographic study reported the tibial cartilage facet to be 8.4 ± 2.1 mm posterior and superior to the anterior-most radiographically discernible point of the tibial plafond. The authors recognize that these landmarks and distances may not be directly comparable as anatomically visible and physically palpable landmarks may not directly coincide with what is radiographically identifiable; however, similarities between these measurements suggests

that the anatomic structures were consistently identified across studies.

Likewise, agreement between previous anatomic descriptions and radiographic measurements presented here were also found for the commonly injured AITFL. Williams et al. [44] reported that the AITFL originated on the tibia 9.3 mm (95 % CI 8.6, 10.0) superior to the anterolateral corner of the tibial plafond and inserted on the fibula

Table 8 Radiographic measurements of the interosseous tibiofibular ligament and tibiofibular contact zone, mortise view

	Absolute distance (mm) Mean \pm SD	Directionality (mm) ^a	
		Lateral(+)/medial(-) Mean	Superior(+)/inferior(-) Mean
<i>Interosseous tibiofibular ligament</i>			
Width of ligament attachment (proximal \rightarrow distal)			
Tibial attachment	34.0 \pm 7.8	0.9	-34.2
Fibular attachment	31.0 \pm 5.8	-0.7	-30.7
Tibial attachment to tibial plafond (along superior–inferior axis)			
Proximal terminus	45.0 \pm 9.9	0.0	-45.0
Distal terminus	11.1 \pm 3.5	0.0	-11.1
Fibular attachment to inferior tip of the lateral malleolus			
Proximal terminus	59.0 \pm 6.8	8.2	-58.1
Distal terminus	29.6 \pm 3.4	10.5	-27.4
<i>Tibiofibular contact zone</i>			
Tibial cartilage facet to lateral tibial plafond	2.3 \pm 1.2	-1.9	0.2
Fibular cartilage facet to inferior tip of the lateral malleolus	22.8 \pm 2.6	10.3	-20.2

^a Directionality components were averaged and reported for each measurement starting from each respective attachment to the landmark of interest

5.8 mm (95 % CI 4.4, 7.3) proximal to the anteromedial (Wagstaffe's) tubercle [44]. On the lateral radiographic view, the present study found the AITFL tibial attachment was 9.6 ± 1.5 mm superior and slightly posterior to the anterior corner of the tibial plafond and the centre of the fibular footprint was 4.4 ± 1.7 mm superior and posterior to the anterior-most point of the anterior fibular tubercle. These findings are evidence of strong agreement between anatomic and radiographic descriptions.

These radiographic guidelines have immediate and direct applications to anatomic reduction, surgical repair, or reconstruction following syndesmosis injuries. To date, surgical fixation and reconstruction techniques following syndesmotic injuries have been described for in vivo repairs as well as in cadaveric models [4, 9, 14, 21, 26, 28, 30, 32, 42, 45, 47]. In the case series reported, there are varying levels of success and a wide array of complications. In the case of acute syndesmosis injuries with instability, anatomic reduction via indirect transosseous fixation, either by syndesmotic screws or cortical button-suture constructs, is the current standard surgical practice [3, 24, 26, 32, 46]. The current literature recommends that such fixation devices be placed between 2 and 5 cm proximal to the tibial plafond in line with the neutral tibiofibular orientation to avoid malreduction of the syndesmosis [32]. Despite these recommendations, malreduction is a frequently reported clinical complication, particularly with the use of syndesmotic screws [9, 25, 30, 42]. The incidence of malreduction with syndesmosis screw fixation has been reported to be as high as 52 % [12]. Fortunately, there is evidence that screw removal or screw breakage can lead to spontaneous

reduction and improved symptoms in a high percentage of patients [15, 22, 40]. However, this suggests that ensuring initial anatomic reduction and fixation might lead to improved results including fewer broken screws or those requiring removal. The present study recommends that fixation screws or suture-button fixation devices be placed at a minimum of 12.4 mm and no more than 45.9 mm proximal to the tibial plafond on the lateral radiographic view to land within the footprint of the ITFL fibres and to ensure the safety of the synovial recess and articular surfaces. As recommended by previous studies, all devices should be inserted in line with the anatomic tibiofibular plane to avoid malreduction.

In addition to indirect fixation, various anatomic and non-anatomic reconstruction techniques have been described in the literature to address chronic instability, which also may be guided by the radiographic data presented in this study. Beumer et al. [4] initially described a technique in which an attenuated and elongated AITFL was retensioned through a proximal and medializing osteotomy of its tibial insertion. Grass et al. [14] subsequently described a modification of a peroneus longus ligamentoplasty in which a split peroneus longus tendon was threaded through a combination of three fibular and tibial canals to reconstruct the posterior, interosseous, and anterior ligaments of the syndesmosis. More recently, several authors have described free hamstring graft reconstructions including isolated AITFL reconstructions [45], combined AITFL/ITFL [28] and AITFL/PITFL [47], and complete syndesmosis triligamentous reconstructions [21]. Regardless of surgical technique, the radiographic guidelines defined

in the present study could be utilized intraoperatively to guide the placement of reconstruction tunnels and fixation devices and to assess graft placement postoperatively. Specifically, the authors advocate that AITFL reconstruction tunnels be placed 9.6 mm superior and slightly posterior to the anterior-most radiographic aspect of the tibial plafond and 4.4 mm superior and posterior to the anterior fibular tubercle on the lateral view. Similar recommendations could be made for ITFL and PITFL reconstruction tunnels based on lateral and mortise measurements described in the present study. However, the authors would like to emphasize that such recommendations should be synthesized in conjunction with previously published gross anatomic data. Furthermore, suggested alterations in surgical technique in light of the presented radiographic data have not yet been evaluated biomechanically or clinically.

Clinical outcomes have often been reported to be satisfactory for both transosseous fixation and reconstruction; however, complications have also been reported including malreduction, residual diastasis, loss of range of motion (decreased dorsiflexion), and continued progression of degenerative joint disease [9, 14, 28–30]. Multivariate regression analysis of clinical outcomes has identified non-anatomic reduction (malreduction) as the only variable to independently influence patient outcomes [30]. Malreduction and failure to restore native joint contact mechanics is of particular clinical concern because previous biomechanical research has demonstrated that syndesmotic instability and widening of the ankle mortise, allowing for as little as 1 mm of relative lateral displacement of the talus, alters joint contact kinematics and reduces tibiotalar contact areas by as much as 42 % [36]. In addition to reduced contact areas, similar research has demonstrated that injuries resulting in altered tibiotalar contact mechanics significantly increase peak tibiotalar contact pressures [41]. It is believed that such non-physiologic contact areas and pressures can lead to subsequent chondral damage and arthritic changes [35]. The authors believe that the defined radiographic parameters presented here may facilitate fidelity to anatomic-based techniques and optimize the restoration of native syndesmosis joint kinematics postoperatively.

The authors acknowledge some limitations of the present study. This study utilized 12 cadaveric foot and ankle specimens. Given the relatively small sample size, the range of distances observed in this study may not represent the variability observed across a larger population. However, the number of specimens was comparable to previous radiographic landmark investigations [16, 20, 33, 34, 43]. Data were also comparable to previous anatomic literature [1, 10, 44]. In addition, specimens were generally obtained from older individuals that would fall outside of the typical age cohort that would undergo surgical syndesmotic fixation. However, specimens were screened for bone quality,

osteophyte formation, joint space narrowing, and gross anatomic abnormalities. Based on these exclusion criteria, the authors are confident in the radiographic relationships established by this study. The authors also acknowledge that specimens were cut at the midshaft of the tibia and fibula, which may have altered the anatomic orientation of the syndesmosis; however, rigid screw fixation was utilized prior to removal of soft tissue to minimize any deviations from an anatomically accurate position. Finally, the reported measurements are two-dimensional quantitative descriptions of structures with three-dimensional relationships and therefore are subject to potential variability with rotation of the extremity. Therefore, careful adherence to the image acquisition protocol outlined in the materials and methods section is required to obtain results consistent with data presented in this study. Furthermore, the authors recommend that intraoperative navigation and surgical decision-making should always be made in conjunction with gross anatomic information detailing other anatomic soft tissue relationships.

This study provides a comprehensive description of the radiographic anatomy of the ankle syndesmosis, including ligament attachments and articular surfaces. This information will assist in the interpretation of radiographic assessments of the syndesmosis from diagnosis through postoperative follow up. Such guidelines may be particularly useful in more difficult revisions or cases with significant concomitant injury where other means of assessment and navigation may not be easily applied.

Conclusions

In the present descriptive laboratory study, qualitative and quantitative radiographic parameters characterizing relevant ligament attachment sites and cartilage surfaces of the ankle syndesmosis were defined with excellent reliability and reproducibility. In conjunction with current anatomic data, these radiographic guidelines will augment current clinical radiographic diagnostic techniques, improve preoperative planning, assist with intraoperative identification of native anatomy, and facilitate objective postoperative assessment of anatomic-based reduction, repair, and reconstruction techniques.

References

1. Bartonicek J (2003) Anatomy of the tibiofibular syndesmosis and its clinical relevance. *Surg Radiol Anat* 25(5–6):379–386
2. Bassett FH III, Gates HS III, Billys JB, Morris HB, Nikolaou PK (1990) Talar impingement by the anteroinferior tibiofibular ligament. A cause of chronic pain in the ankle after inversion sprain. *J Bone Joint Surg Am* 72(1):55–59

3. Bava E, Charlton T, Thordarson D (2010) Ankle fracture syndesmosis fixation and management: the current practice of orthopedic surgeons. *Am J Orthop* 39(5):242–246
4. Beumer A, Heijboer RP, Fontijne WP, Swierstra BA (2000) Late reconstruction of the anterior distal tibiofibular syndesmosis: good outcome in 9 patients. *Acta Orthop Scand* 71(5):519–521
5. Beumer A, van Hemert WL, Niesing R, Entius CA, Ginai AZ, Mulder PG, Swierstra BA (2004) Radiographic measurement of the distal tibiofibular syndesmosis has limited use. *Clin Orthop Relat Res* 423:227–234
6. Bonnin JG (1970) Injuries to the ankle. Hafner Pub. Co., Darien
7. Boytim MJ, Fischer DA, Neumann L (1991) Syndesmotic ankle sprains. *Am J Sports Med* 19(3):294–298
8. Candal-Couto JJ, Burrow D, Bromage S, Briggs PJ (2004) Instability of the tibio-fibular syndesmosis: have we been pulling in the wrong direction? *Injury* 35(8):814–818
9. Davidovitch RI, Weil Y, Karia R, Forman J, Looze C, Liebergall M, Egol K (2013) Intraoperative syndesmotic reduction: three-dimensional versus standard fluoroscopic imaging. *J Bone Joint Surg Am* 95(20):1838–1843
10. Ebraheim NA, Taser F, Shafiq Q, Yeasting RA (2006) Anatomical evaluation and clinical importance of the tibiofibular syndesmosis ligaments. *Surg Radiol Anat* 28(2):142–149
11. Ebraheim NA, Lu J, Yang H, Mekhail AO, Yeasting RA (1997) Radiographic and CT evaluation of tibiofibular syndesmotic diastasis: a cadaver study. *Foot Ankle Int* 18(11):693–698
12. Gardner MJ, Demetrakopoulos D, Briggs SM, Helfet DL, Lorich DG (2006) Malreduction of the tibiofibular syndesmosis in ankle fractures. *Foot Ankle Int* 27(10):788–792
13. Gerber JP, Williams GN, Scoville CR, Arciero RA, Taylor DC (1998) Persistent disability associated with ankle sprains: a prospective examination of an athletic population. *Foot Ankle Int* 19(10):653–660
14. Grass R, Rammelt S, Biewener A, Zwipp H (2003) Peroneus longus ligamentoplasty for chronic instability of the distal tibiofibular syndesmosis. *Foot Ankle Int* 24(5):392–397
15. Hamid N, Loeffler BJ, Braddy W, Kellam JF, Cohen BE, Bosse MJ (2009) Outcome after fixation of ankle fractures with an injury to the syndesmosis: the effect of the syndesmosis screw. *J Bone Joint Surg Br* 91(8):1069–1073
16. Haytmanek CT, Williams BT, James EW, Campbell KJ, Wijdicks CA, LaPrade RF, Clanton TO (2015) Radiographic identification of the primary lateral ankle structures. *Am J Sports Med* 43(1):79–87
17. Hopkinson WJ, St Pierre P, Ryan JB, Wheeler JH (1990) Syndesmosis sprains of the ankle. *Foot Ankle* 10(6):325–330
18. Hsu AR, Gross CE, Lee S (2013) Intraoperative O-arm computed tomography evaluation of syndesmotic reduction: case report. *Foot Ankle Int* 34(5):753–759
19. Hunt KJ, George E, Harris AH, Dragoo JL (2013) Epidemiology of syndesmosis injuries in intercollegiate football: incidence and risk factors from National Collegiate Athletic Association injury surveillance system data from 2004–2005 to 2008–2009. *Clin J Sports Med* 23(4):278–282
20. Johannsen AM, Anderson CJ, Wijdicks CA, Engebretsen L, LaPrade RF (2013) Radiographic landmarks for tunnel positioning in posterior cruciate ligament reconstructions. *Am J Sports Med* 41(1):35–42
21. Lui TH (2010) Tri-ligamentous reconstruction of the distal tibiofibular syndesmosis: a minimally invasive approach. *J Foot Ankle Surg* 49(5):495–500
22. Manjoo A, Sanders DW, Tieszer C, MacLeod MD (2010) Functional and radiographic results of patients with syndesmotic screw fixation: implications for screw removal. *J Orthop Trauma* 24(1):2–6
23. Marmor M, Hansen E, Han HK, Buckley J, Matityahu A (2011) Limitations of standard fluoroscopy in detecting rotational malreduction of the syndesmosis in an ankle fracture model. *Foot Ankle Int* 32(6):616–622
24. McBryde A, Chiasson B, Wilhelm A, Donovan F, Ray T, Bacilla P (1997) Syndesmotic screw placement: a biomechanical analysis. *Foot Ankle Int* 18(5):262–266
25. Miller AN, Barei DP, Iaquinio JM, Ledoux WR, Beingessner DM (2013) Iatrogenic syndesmosis malreduction via clamp and screw placement. *J Orthop Trauma* 27(2):100–106
26. Miller RS, Weinhold PS, Dahners LE (1999) Comparison of tricortical screw fixation versus a modified suture construct for fixation of ankle syndesmosis injury: a biomechanical study. *J Orthop Trauma* 13(1):39–42
27. Montagne J, Chevrot A, Galmiche JM, Chafetz N (eds) (1983) Atlas of foot radiology. Mason Publishing, New York
28. Morris MW, Rice P, Schneider TE (2009) Distal tibiofibular syndesmosis reconstruction using a free hamstring autograft. *Foot Ankle Int* 30(6):506–511
29. Mukhopadhyay S, Metcalfe A, Guha AR, Mohanty K, Hemmadi S, Lyons K, O'Doherty D (2011) Malreduction of syndesmosis—are we considering the anatomical variation? *Injury* 42(10):1073–1076
30. Naqvi GA, Cunningham P, Lynch B, Galvin R, Awan N (2012) Fixation of ankle syndesmotic injuries: comparison of tightrope fixation and syndesmotic screw fixation for accuracy of syndesmotic reduction. *Am J Sports Med* 40(12):2828–2835
31. Nielson JH, Gardner MJ, Peterson MG, Sallis JG, Potter HG, Helfet DL, Lorich DG (2005) Radiographic measurements do not predict syndesmotic injury in ankle fractures: an MRI study. *Clin Orthop Relat Res* 436:216–221
32. Phisitkul P, Ebinger T, Goetz J, Vaseenon T, Marsh JL (2012) Forceps reduction of the syndesmosis in rotational ankle fractures: a cadaveric study. *J Bone Joint Surg Am* 94(24):2256–2261
33. Pietrini SD, LaPrade RF, Griffith CJ, Wijdicks CA, Ziegler CG (2009) Radiographic identification of the primary posterolateral knee structures. *Am J Sports Med* 37(3):542–551
34. Pietrini SD, Ziegler CG, Anderson CJ, Wijdicks CA, Westerhaus BD, Johansen S, Engebretsen L, LaPrade RF (2011) Radiographic landmarks for tunnel positioning in double-bundle ACL reconstructions. *Knee Surg Sports Traumatol Arthrosc* 19(5):792–800
35. Rammelt S, Zwipp H, Grass R (2008) Injuries to the distal tibiofibular syndesmosis: an evidence-based approach to acute and chronic lesions. *Foot Ankle Clin* 13(4):611–633
36. Ramsey PL, Hamilton W (1976) Changes in tibiotalar area of contact caused by lateral talar shift. *J Bone Joint Surg Am* 58(3):356–357
37. Sagi HC, Shah AR, Sanders RW (2012) The functional consequence of syndesmotic joint malreduction at a minimum 2-year follow-up. *J Orthop Trauma* 26(7):439–443
38. Shrout PE, Fleiss JL (1979) Intraclass correlations: uses in assessing rater reliability. *Psychol Bull* 86(2):420–428
39. Sikka RS, Fetzer GB, Sugarman E, Wright RW, Fritts H, Boyd JL, Fischer DA (2012) Correlating MRI findings with disability in syndesmotic sprains of NFL players. *Foot Ankle Int* 33(5):371–378
40. Song DJ, Lanzl JT, Groth AT, Drake M, Orchowski JR, Shaha SH, Lindell KK (2014) The effect of syndesmosis screw removal on the reduction of the distal tibiofibular joint: a prospective radiographic study. *Foot Ankle Int* 35(6):543–548
41. Thordarson DB, Motamed S, Hedman T, Ebramzadeh E, Bakshian S (1997) The effect of fibular malreduction on contact pressures in an ankle fracture malunion model. *J Bone Joint Surg Am* 79(12):1809–1815

42. Westermann RW, Rungprai C, Goetz JE, Femino J, Amendola A, Phisitkul P (2014) The effect of suture-button fixation on simulated syndesmotic malreduction: a cadaveric study. *J Bone Joint Surg Am* 96(20):1732–1738
43. Wijdicks CA, Griffith CJ, LaPrade RF, Johansen S, Sunderland A, Arendt EA, Engebretsen L (2009) Radiographic identification of the primary medial knee structures. *J Bone Joint Surg Am* 91(3):521–529
44. Williams BT, Ahrberg AB, Goldsmith MT, Campbell KJ, Shirley L, Wijdicks CA, LaPrade RF, Clanton TO (2015) Ankle syndesmosis: a qualitative and quantitative anatomic analysis. *Am J Sports Med* 43(1):88–97
45. Yasui Y, Takao M, Miyamoto W, Innami K, Matsushita T (2011) Anatomical reconstruction of the anterior inferior tibiofibular ligament for chronic disruption of the distal tibiofibular syndesmosis. *Knee Surg Sports Traumatol Arthrosc* 19(4):691–695
46. Zalavras C, Thordarson D (2007) Ankle syndesmotic injury. *J Am Acad Orthop Surg* 15(6):330–339
47. Zamzami MM, Zamzam MM (2009) Chronic isolated distal tibiofibular syndesmotic disruption: diagnosis and management. *Foot Ankle Surg* 15(1):14–19